Zhuli Yang[1],
Fumei Wang[2]*,
Fuwang Guan[1],
Jin Luo[2],
Yiping Qiu[1],
Chuyang Zhang[1]

Interfacial Structure of Polytrimethylene Terephthalate/Polyethylene Terephthalate Bicomponent Filament

DOI: 10.5604/01.3001.0015.6465

[1] Quanzhou Normal University, College of Textiles and Apparel, Quanzhou, Fujian 362000, People's Republic of China

[2] Donghua University, Ministry of Education, Key Laboratory of Textile Science & Technology, Shanghai 201620, People's Republic of China, e-mail: wfumei@dhu.edu.cn

Abstract
The interfacial structure and binding forces of polytrimethylene terephthalate/polyethylene terephthalate filament were investigated through the methods of Carbon-13 nuclear magnetic resonance (^{13}C-NMR), differential scanning calorimeter (DSC), scanning electron microscopy (SEM) and optical microscopy. When two molten polymers met during the spinning process, an interface layer between the PTT and PET components formed and played an important role in binding the two components together. When the blending time was sufficient, an ester-interchange reaction took place with the generation of the copolymer. The PET recrystallisation was observed in the DSC curve under the influence of entangled PTT molecular chains. The morphology of the cross-section and side view proved that the linear boundary line was short and weaker in binding without a chemical bond and molecular diffusion. Side-by-side bi-component fiber and split-type fiber was able to be controllably spun by adjusting the spinning parameters.

Key words: *PTT/PET, interface, copolymer, crystallisation, morphology.*

Introduction

Polytrimethylene terephthalate/polyethylene terephthalate (PTT/PET) side-by-side bi-component filament is produced via melt spinning by means of a twin-screw extruder [1, 2]. Interfaces between the PTT and PET component play a key role in combining the two components together and keeping a side-by-side structure. Gaining insight into the interfacial structure will enhance our ability to design a materials system with controlled adhesion, split, and elasticity characteristics [3]. Recent experimental evidence indicates that PTT/PET interactions can drastically influence the quality of products obtained by melt processing operations, such as extrusion and cooling [4-6].

PTT has been used as environmentally friendly material because 1,3-propandiol, which is the raw material of PTT, can be made by biological fermentation [7-8]. PTT/PET filament and the PTT/PET blend have received great scientific and industrial interest. These studies have included spinning technology [9, 10], elasticity [9, 11], crimp structure [12, 13], textile use [9, 11-13] etc. In other studies, the PTT/PET blend was proved to be a thermodynamically compatible system [14-18]. Xiao [14] and Liang [15] found that PTT/PET blends are miscible in amorphous areas and partially so in crystalline regions. Son [16], Shyr [17] and many other scholars [18-22] found that in the PTT/PET blend system an ester exchange reaction took place, and a copolymer was produced near or above the melting points. Some researchers studied the sequential structure of copolymer [20], as well as the crystallisation behavior of the blend system [21]. However, due to structural similarity and transesterification between PTT and PET, there was no interface in PTT/PET blends [16].

Existing researches mostly focus on PTT/PET solution blends and melt blends, with studies on the PTT/PET interface layer being rarely. For PTT/PET filament, its interfacial structure is distinct from that of PTT/PET blends. Multicomponent coextrusion provides the possibility to combine PTT and PET components with diverging properties into a composite extrudate, which shows a new set of attributes that have not been obtained previously [23]. Kikutani [24] proved that the structure development of one component is strongly influenced by the viscosity and solidification temperature of another during the melt spinning of bicomponent fiber. The formation of an interfacial adhesion layer will be influenced by the temperature, molecular weight, chain orientation, polydispersity and molecular structure of polymers [25, 26]. Also, the polymer-polymer compatibility system has a direct relation to the interfacial affinity [27]. Southern tried to enhance the interfacial interactions between components in melt-spun materials through the formation of mechanical interlocking [28]. Ide and Hasegawa enhanced the compatibility of polymer blends through the grafted polymer [29]. Various authors have analysed the interface of fiber-matrix, which provide better references [30].

This work focusses on the interfacial structure between PTT and PET components in PTT/PET side-by-side filament. The interfacial interaction in bi-component coextrusion filament, including the chemical bond, physical interlocking and crystallisation behavior, were analysed through nuclear magnetic resonance, thermal and morphological analysis.

Materials and experiments

Materials

The PTT/PET filaments selected in this work are the most familiar and most used, the basic parameters of which are listed in ***Table 1***. Filament C is the one with which PTT and PET components were separated in a previous study [4, 5]. ***Table 2*** shows the molecular structure of PTT/PET copolymer.

Table 1. *Specifications of samples.* ***Note:*** **FDY, full draw yarn; DTY, draw texturing yarn; *DPF, denier per filament; *D, denier, unit of fineness.*

Filament	Structure	Fineness, D*	DPF*, D	Cross-Section shape	Volume ratio
A	FDY*	150	2.60	Pear-shaped	50/50
B	FDY		3.47	Dog-bone-shaped	50/50
C	DTY		2.31	Dog-bone-shaped	50/50

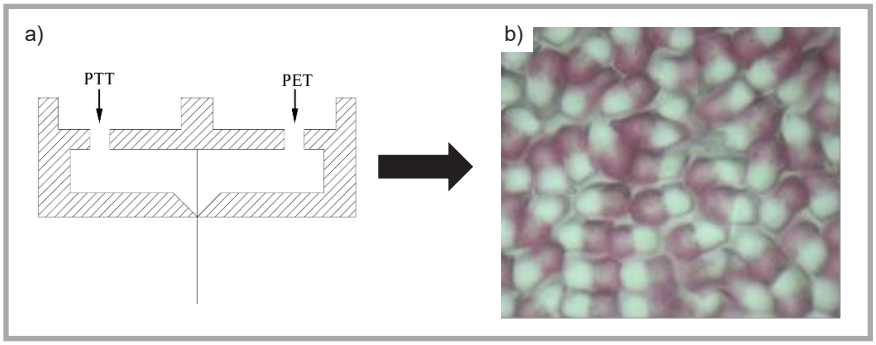

Figure 1. *Formation of interface layer: a) spinneret, b) cross sections of dyed PTT/PET filament.*

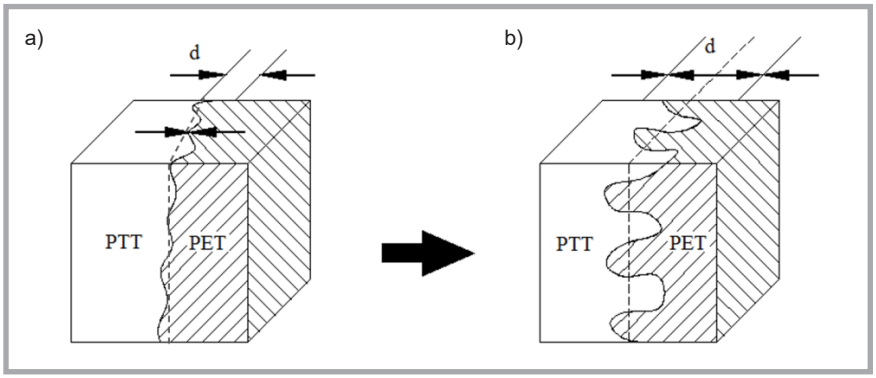

Figure 2. *Model of interface layer: a) meet of two molten polymers, b) diffusion of molecular chains.*

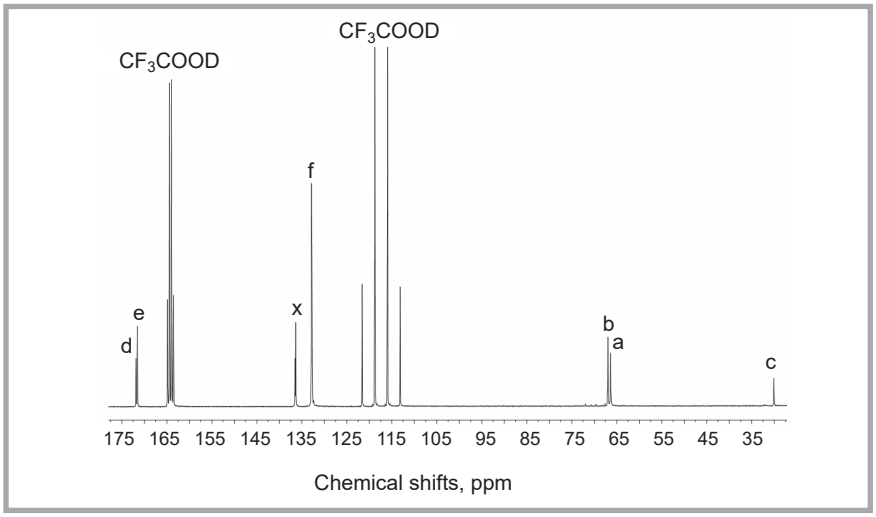

Figure 3. *^{13}C-NMR spectrogram of PTT/PET Filament A.*

Table 2. *Structures of PTT/PET copolymer.*

Polymer	Molecular structure
PET	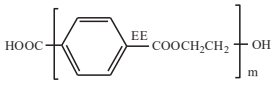
PTT	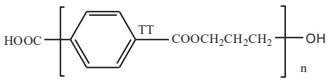
Copolymer	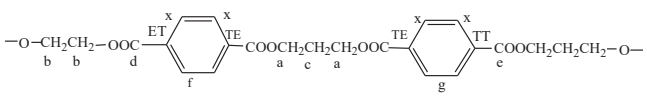

Experiments

Differential scanning calorimeter test

A differential scanning calorimeter (DSC, Pyris 1, Perkin-Elmer Cetus Corporation, USA) was used to study the crystallisation behavior of PTT/PET filament along with standard aluminum pans under a nitrogen atmosphere. Approx. 5 mg samples were heated at a rate of 10 °C/min from ambient temperature to 300 °C.

Nuclear magnetic resonance test

A carbon-13 nuclear magnetic resonance (^{13}C-NMR) test was conducted by means of a NMR spectrometer (Bruker Avance 400, BRUKER, Swiss) at 100.6 MHz. Approx. 100 mg samples were dissolved in 0.6 ml deuterated trifluoroaectic acid. The production of copolyester was measured from the area of the signal peaks.

Scanning electron microscope test

Scanning electron microscope (SEM TM3000, Hitachi, Japan) micrographs were used to study the cross-section morphology of three different samples. The cross-sections were prepared by means of Hardy's cross-sectional device (Y172) and sputter coated with a thin layer of gold, prior to SEM investigation.

Optical Microscope test

The optical microscope images (LABOMED, Labo America, Inc. USA) were used to study the cross-section and longitudinal morphology.

Results and discussion

Generation of Interface Layer

Dried PTT and PET chips were spun using the same spinneret plate after heating in a twin-screw extruder (in ***Figure 1.a***). As Shown in ***Figure 1.b***, there is an interface between the two polymers in the cross-section view. Actually, it is not only an interface line but an interface layer which is generated after being co-extruded. The formation occurs after the meeting of two polymer melts and the consequent diffusion of PTT and PET molecular chains [31]. The interface layer of the PTT/PET filament is composed of a boundary line and two side diffusive parts. Therefore, the interface layer works as a micro blending system. In this micro-system, PTT and PET molecular chains diffuse and entangle together.

A model of the interface layer is shown in ***Figure 2*** (*d* is the thickness of inter-

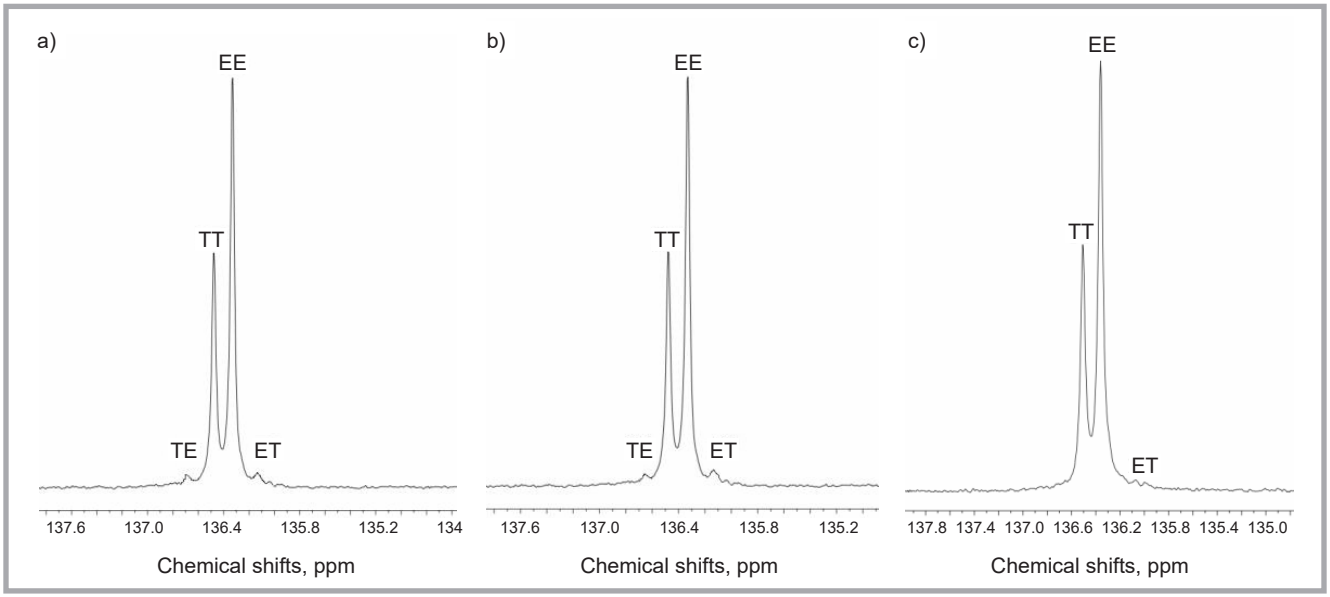

Figure 4. *^{13}C-NMR spectrogram of copolymer: a) Filament A, b) Filament B, c) Filament C.*

face layer). The thickness of the interface layer is closely connected with the compatibility of the two polymers. Due to the interdiffusion of molecular chains, *d* between two immiscible polymers is very thin [32]. When the compatibility of the two polymers increases, their adhesion increases, and there is no clear interface.

Interaction forces of interface layer

As a micro-system, the interface layer plays an important role in the combination of two components. There are two bonding patterns between molecules in the interface layer. The first one is a chemical bond, which is mostly a covalent bond. A physical bond, involving molecule diffusion, recrystallisation and Van der Waal's force, is the second bonding pattern.

Chemical bond

Many studies have reported that an ester-interchange reaction occurs in PTT/PET blends [16-18]. The ^{13}C-NMR spectrograms are shown in ***Figure 3*** and ***Figure 4***. The smaller characteristic peaks near 136.2 and 136.6 ppm (ET and TE) indicate the existence of copolymer, which provides strong binding between PTT and PET components. It also proves that a reversible ester-ester interchange reaction occurred in the interface layer due to the residual catalyst present in commercial PET and PTT during the melting process [33, 34].

The absorption peak areas could give an explanation of the covalent bond quantitatively [35]. ***Figure 4*** shows that the peaks of three PTT/PET filaments are different and that filament C has very little copolymer. More copolymer in Filaments A and B means stronger chemical bonding than that of filament C. It was reported that the resonance intensity of the peak increases with the increasing of the blending time [22]. The little production of copolymer in filament C is attributed to the less blending time.

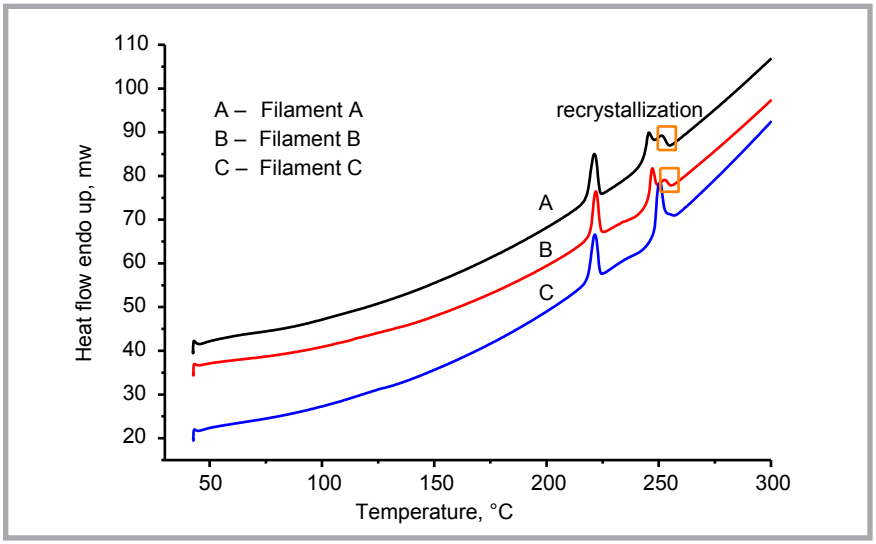

Figure 5. *DSC curves of PTT/PET filament.*

Table 3. *Melting points and melting enthalpy.*

Samples	Melting points, °C			Melting enthalpy, J·g^{-1}		
	PTT	PET	Copolymer	PTT	PET	Copolymer
Filament A	221.93	246.83	252.73	19.75	20.43	0.88
Filament B	221.92	247.15	252.39	25. 08	26.16	1.30
Filament C	221.62	250.12	–	21.43	30.98	–

Physical bond

The DSC test was adopted to study the crystallisation behaviour of PTT/PET filaments. In ***Figure 5***, the small endothermic melting peak at 252 °C is the recrystallisation of PET components [21, 36]. The cold-crystallisation temperature of PTT (63-85 °C) is lower than that of thePET component (130-170 °C). Therefore, the crystallisation of PET is prioritised because of its higher crystal-

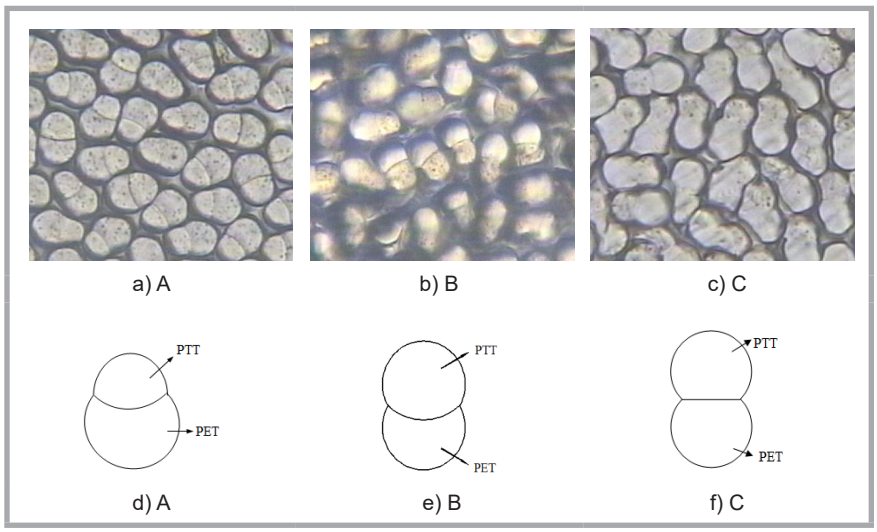

Figure 6. *Optical microscopy images and diagrams of PTT/PET filaments' cross-section.*

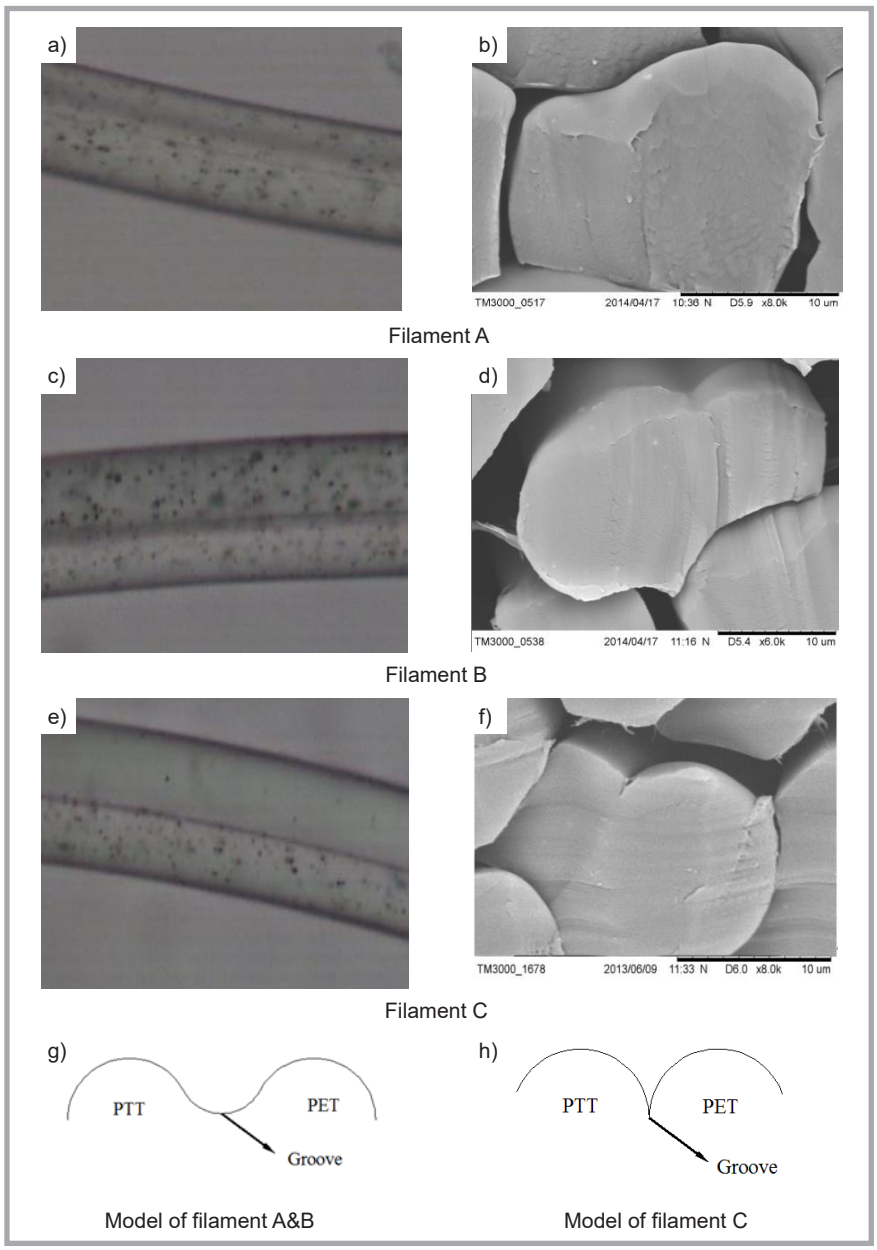

Figure 7. *Optical morphology images of side view (a, c, e), SEM images (b, d, e) and diagram (g, f) of the cross-sections.*

lisation temperature, followed by PTT. The entanglement of PTT and PET chains in the interface layer retards the crystallisation of PET near and in the interface layer. Therefore, PET far from the interface crystallises firstly and works as a crystal nucleus. PET near the interface layer crystallises on the PET nucleus, and recrystallisation is generated due to the influence of PTT chains [19]. The crystallisation of PET is slower because of its rigid molecular chain. Due to the "Z" macromolecule chain, the crystallization of PTT is a magnitude faster [37] and appears unaffected. The production of recrystallisation gives expression to molecular diffusion and entanglement. Meanwhile, the entangled PTT and PET molecular chains are interlocked by recrystallisation, like transcrystallization in composite material. Therefore, recrystallisation can strengthen the binding between PTT and PET.

The production of recrystallisation of filaments A and B is more than that of filament C (in ***Figure 5***), bringing more physical bonding. With a less covalent bond and recrystallisation, the PTT and PET components in filament C are combined mainly by the Van der Waals force. Consequently, they separated easily by the external force in an alkali environment [4-5].

Morphology

Morphology of cross-section

Made up of entangled molecules, the supermolecular structure and polymer density of the interface layer is clearly different from those of the PTT and PET single component [32]. For instance, the interface layer has distinct transparency. In ***Figure 6***, a clear interface line can be observed in filaments A and B. filament C has no boundary line, revealing that the interface layer of filament C is much thinner and that some cross-sections have almost no interlayers.

In ***Figure 6***, the interface lines of filaments A and B curve, while the boundary in filament C is almost straight. This is caused by the viscosity difference between PTT and PET [11, 38]. When the two components meet earlier or the spinning temperature is higher, the viscosity difference is larger and a crescent boundary takes shape. The crescent-shape bows over the component with smaller intrinsic viscosity (***Figure 6.d*** and ***6.e***). In this case, there is enough time for PTT and

PET to blend. The diffused and tangled molecular chains stimulate the generation of copolymer and recrystallisation. Therefore, the interface layer thickness and interfacial bonding are larger. Reversely, when the two components meet late or the temperature is lower, a linear boundary forms (***Figure 6.g***).

The cross-sectional dimensions in ***Table 4*** show that the average width of filament C is only 12.12 μm. while the width of filaments A and B are 16.14 μm and 17.11 μm, respectively. Due to the linear boundary line, the width of Filament C is approximately equal to the length of the boundary line. Because of the arc-shaped boundary, the boundary length of filaments A and B is longer than the width. The shortest and linear boundary line of filament C also demonstrates the weaker component bonding of filament C.

Morphology of side view

Figure 7 shows the cross-sections and side views of three PTT/PET filaments. The longitudinal grooves of filaments A and B are wide and in a circular arc form, while that of filament C is in a narrow and slit form. These grooves are side views of the interface layer. It also proves that the interface layer of filament C is very thin, which will result in component separation under an external force and alkali treatment.

Conclusions

An interface layer between PTT and PET components forms during coextrusion, working as a micro blend system. An ester-interchange reaction occurs with the generation of copolymer in the interface layer. Without sufficient blending, the production of copolymer of filament C is little but still exists, which provides a less chemical bond for the binding of components.

The crystallisation of PET in the interface layer is retarded by the entangled PTT molecular chains, which causes the generation of recrystallisation. The entangled PTT and PET chains are interlocked together by recrystallisation. Filament C has very little recrystallisation and less physical interlocking.

Blending time has a great influence on the interfacial structure. An arc-shaped boundary line forms through coextrusion and the interface layer provides a sufficient combination. Conversely, without sufficient mixing, component separation occurs under the external force and alkali treatment, which would be a new method for making ultrafine fibers for compatible polymers.

Table 4. *Dimension of cross-section.*

	Filament A		Filament B		Filament C	
	Length	Width	Length	Width	Length	Width
Average, μm	19.65	16.14	25.58	17.11	22.04	12.12
CV, %	4.79	5.64	5.57	6.05	4.15	6.21

Acknowledgements

This work was supported by the Startup Foundation for Doctors of Quanzhou Normal University (Grant No. H18024 & H18028), the Education and Scientific Research Foundation for Middle-aged and Young Scientist of Fujian Province, China (JT180377), the Quanzhou Home-bay Recruitment Program of Global Talents (2017ZT002),the Quanzhou City Science & Technology Program of China (2020C039R, 2018K002), and the Natural Science Foundation of Fujian Province, China (Grant No. 2019J01740).

References

1. Rwei SP, Lin YT, Su YY. Study of Self--Crimp Polyester Fibers. *Polymer Engineering and Science* 2005; 45(6), 838-845.
2. Jeffries R. Bi-Component Fiber. Merrow Publishing Co. Ltd, Manchester, 1971.
3. Kevin FM, Doros NT. Interfacial Structure and Dynamics of Macromolecular Liquids: A Monte Carlo Simulation Approach. *Macromolecules* 1989; 22(7): 3143-3152.
4. Yang ZL, Wang FM. Dyeing and Finishing Performance of Different PTT/PET Bi-Component Filament Fabrics. *Indian Journal of Fiber & Textile Research* 2016; 41(4), 422-417.
5. Yang ZL, Xu BG, Wang FM. Key Factors Affecting Binding Tightness Between Two Components Of PTT/PET Side-By--Side Filaments. *Industria Textila 2016;* 67(4): 226-232.
6. Chuah HH. Orientation and Structure Development in Poly (Trimethylene Terephthalate) Tensile Drawing. *Macromolecules 2001;* 34(20): 6985-6993.
7. Drozdzynska A, Leja K, Czaczyk K. Biotechnological Production Of 1,3-Propanediol from Crude Glycerol. *Biotechnologia* 2011; 92(1): 92-100.
8. Deckwer WD. Microbial Conversion of Glycerol to 1,3-Propanediol: Recent Progress. FEMS Microbiology Reviews 1996; 16(2-3): 143-149.
9. Liu XS, Jiao SY, Wang FM. Configuring the Spinning Technology of PTT/PET Bicomponent Filaments According to Fabric Elasticity. *Textile Research Journal* 2013; 83(5): 487-498.
10. Oh TH, Han SS, Lyoo WS, Jeon HY. Molecular Structures and Physical Properties of Heat-Drawn Conjugates Fibers. *Polymer Engineering and Science* 2014; 51(2): 232-236.
11. Gu F, Wang FM. Prediction Method of Elastic Elongation of PTT/PET Self--Crimping Fibers. Journal of Donghua University (Natural Science). 2001; 37(3): 262-266.
12. Luo J, Wang FM, Xu BG. Factors Affecting Crimp Configuration of PTT/PET Bicomponent Filaments. *Textile Research Journal* 2011; 81(5): 538-544.
13. Chen SH, Wang SY. Latent Crimp Behavior of PET/PTT Elastomultieater and a Concise Interpretation. *Journal of Macromolecular Science B-Physics* 2011; 50(7): 1447-1459.
14. Xiao CX, Li WG, Huang XA. Research on the Compatibility of PTT/PET Blends. *Synthesis Fiber* 2003; 32(6): 22-25.
15. Liang H, Wu W, Qian Q, Liu M. Melting Crystallization of PET/PTT Blends. *Polymer Material Science & Engineering* 2007; 23(1): 153-156.
16. Son TW, Kim KI, Kim NH. Thermal Properties of Poly (Trimethylene Terephthalate)/Poly(Ethylene Terephthalate) Melt Blends. *Fiber and Polymer* 2003; 4(1): 20-26.
17. Shyr TW, Lo CM, Ye SR. Sequence Distribution and Crystal Structure of Poly(Ethylene/Trimethylene Terephthalate) Copolyesters. *Polymer* 2005; 46(14): 5284-5298.
18. Chiu FC, Huang KH, Yang JC. Miscibility and Thermal Properties of Melt-Mixed Poly(Tremethylene Terephthalate)/ Amorphous Copolyester Blends. *Journal of Polymer Science: Part B: Polymer Physics* 2003; 41(19): 2264-2274.
19. Pan JJ, Wang YF, Li BH, Run MT. Phase Morphology, Mechanical and Thermal Properties of Poly(Trimethylene Terephthalate) and Poly(Ethylene Terephthalate) Blends. *Applied Mechanics and Materials* 2016; 835: 277-283.
20. Cui J, Wang CS, Wang HP, Chen Y, Zhang YM. Sequence Distribution and Structure of PTT/PET Copolyesters. *Synth Fiber*. 2006; 35(9): 1-5.
21. Li GJ, Xing DG, Li W, Lu KX, Chen YM, Huang NX, Zhou EL. Studies on the morphology and crystallization behavior of PTT/PET blend system. Acta Polymerica Sinica. 2005; 5: 736-739.
22. Arasteh R, Naderi A, Kaptan N, Maleknia L. Effects of fiber spinning on the morphology, rheology, thermal, and mechanical properties of poly(trimethylene terephthalate)/poly(ethylene terephthalate) blends. *Advances in Polymer Technology* 2015; 33, S1.

23. Leal AA, Neururer AO, Bian A, Gooneie A, Rupper P, Masania K, Dransfeld C, Hufenus R. Interfacial Interactions In Bicomponent Polymer Fibers. *Polymer* 2018; 142: 375-386.
24. Kikutani T, Radhakrishnan J, Arikawa S, Takaku A, Okui N, Jin X, Niwa F, Kudo Y. High-Speed Melt Spinning of Bicomponent Fibers: Mechanism of Fiber Structure Development in Poly(Ethylene Terephthalate)/ Polypropylene System. *Journal Of Applied Polymer Science* 1996; 62(11): 1913-1924.
25. Hufenus R, Yan Y, Dauner M, Yan D, Kikutani T. Bicomponent fibers in: Jinlian Hu (Ed.), Handbook of Fibrous Materials, Wiley-VCH Publishing Ltd., 2017.
26. Jablonski EL. Interdiffusion Phenomena at Partially Miscible Polymer Interfaces, Iowa State University, 2002.
27. Spruiell JE, White JL. Structure Development During Polymer Processing-Studies of Melt Spinning of Polyethylene and Polypropylene Fibers. *Polymer Engineering Science* 1975; 15(9): 660-667.
28. Southern JH, Marin DH, Baird DG. Improved Shear-Core Adhesion in Biconstituent Fiber via Interface Mixing. *Textile Research Journa* 1980; 50(7): 411-416.
29. Ide F, Hasegawa A. Studies on Polymer Blend of Nylon-6 and Polypropylene or Nylon-6 and Polystyrene Using Reaction of Polymer. *Journal of Applied Polymer Science* 1974; 18(4): 963-974.
30. Yang XG. Interface of Composite Material. Chemical Industry Press, Beijing; 2010.
31. Wu PX, Zhang LC. Polymer Blending Modification. China Light Industry Press, Beijing, 1994.
32. Chen XH, Peng SX. Principle and Technology of Polymer Blending. Chemical Industry Press, Beijing, 2011.
33. Smith WA, Barlow JW, Paul DR. Chemistry of Miscible Polycarbonate Copolyester Blends. *Journal of Applied Polymer Science* 1981; 26(12): 4233-4265.
34. Antxon MI, Sebastian MG. Chemical Structure and Microstructure of Poly(Alkylene Terephthalate)S, their Copolyesters and their Blends as Studied by NMR. *Macromolecular Chemistry and Physics* 2014; 215(22): 2138-2160.
35. Akitt JW, Mann BE. NMR and Chemistry. Cheltenham, UK: Stanley Thornes, 2000.
36. Chuah HH. Crystallization kinetics of poly(trimethylene terephthalate). *Polymer Engineering and Science* 2001; 41(2): 308-313.
37. Chen GK, Gu LX. Studies on the Crystallization Properties and Crystallization Kinetics of Polytrimethylene Terephthalate. *Polymer Materials Science and Engineering* 2001; 17(1), 141-145.
38. Oh TH, Han SS, Lyoo WS, Jeon HY. Molecular Structures and Physical Properties of Heat-Drawn Conjugates Fibers. *Polymer Engineering and Science* 2014; 51(2): 232-236.

Received 12.11.2020 Reviewed 23.06.2021